# A Finite Element Formulation for Transient Thermal Analysis of Nonlinear Material Problems

D.R.J. Owen
*Department of Civil Engineering, University College of Swansea, Singleton Park, Swansea SA2 8PP, U.K.*
F. Damjanic
*V. Strucni suradnik, Gradj. Institut Zagreb, F.G.S., Split, Yugoslavia*

SUMMARY

Thermal loading of prestressed concrete structures is considered which necessitates the inclusion of time effects in the analysis. The technique described in this paper involves concurrently solving an uncoupled set of equations within a time interval to provide both the displacement and temperature increments. A two level time stepping scheme is employed to predict temperature changes within a time interval and elasto-viscoplastic material analysis is performed using an explicit forward difference scheme incorporating an equilibrium iteration procedure.

A dual criterion for yielding and crushing in terms of stresses and strains is considered which is complemented with a tension cut-off representation.

Numerical computations are presented which indicate that, for thermal loading a full transient thermal-mechanical analysis is sometimes essential in order to obtain a realistic structural response.

## 1. Introduction

The last decade has witnessed rapid advances in the use of finite element methods for the analysis of reinforced concrete structures as reported in several comprehensive review articles [1-5]. Some numerical approaches have been developed to mainly study local behaviours, such as bond effects, cracking, interface shear and dowel action while other numerical studies have been directed at the analysis and design of components and structures. In the present study, an averaging procedure is employed to simulate concrete cracking; with the crack effects being assumed to be distributed within a sampling volume. An average shear modulus which accounts for both crack interface effects and dowel action is employed and a full bond is assumed at the steel-concrete interface.

The technique described in this paper for transient thermal loading problems involves concurrently solving an uncoupled set of equations within a time interval to provide both the displacement and temperature increments. Use of a fully coupled theory is avoided due to lack of appropriate material data, but the sequential approach adopted allows the material properties to be temperature dependent. A two level time stepping scheme with $1/2 \leq \alpha \leq 1$ is employed to predict temperature changes occurring within a time interval. Elasto-viscoplastic material analysis is performed using an explicit forward difference scheme incorporating an equilibrium correction procedure.

## 2. Material modelling

In this section the constitutive behaviour of concrete is described in a form suitable for numerical computation.

### 2.1 Compressive behaviour of concrete

A dependence of the yield function on the mean normal stress $I_1$ and the shear stress invariant $J_2$ can be shown to be adequate for most situations. The following criterion is employed which involves only the definition of two material parameters

$$f(I_1, J_2) = |\beta(3J_2) + \alpha I_1|^{1/2} = \sigma_o \qquad (1)$$

where $\alpha$ and $\beta$ are material parameters and $\sigma_o$ is the equivalent effective stress taken as the compressive stress from a uniaxial test. The parameters $\alpha$ and $\beta$ are determined from the uniaxial and biaxial experimental results of Kupfer [6] giving

$$\alpha = 0.355\ \sigma_o \qquad (2)$$

$$\beta = 1.355$$

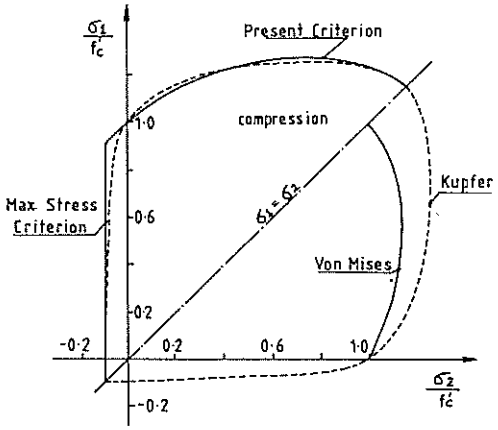


Fig. 1 Compressive yield and tensile cracking criterion for concrete

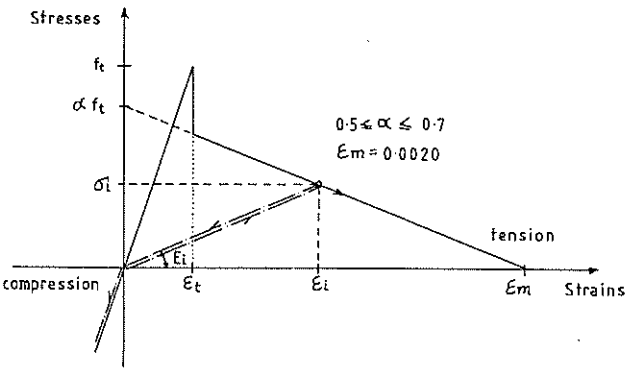


Fig. 2 Tension stiffening model for concrete

This expression is compared in Fig. 1 with the experimental results of Kupfer et al [6] in biaxial stress space. The value of $\sigma_o$ is taken as the ultimate stress $f'_c$ obtained from a uniaxial compression test. An elastic response is assumed up to the effective stress value $\sigma_o = f'_c$, after which a perfectly plastic response follows until the crushing surface is reached.

The crushing type of concrete fracture is a strain controlled phenomenon. The lack of available experimental data on concrete ultimate-deformation capacity under multiaxial stress states has resulted in the appropriate strain criterion being developed by simply converting the yield criterion described in terms of stresses directly into strains. Thus,

$$\beta(3J'_2) + \alpha I'_1 = \varepsilon_u^2 \tag{3}$$

where $I'_1$ and $J'_2$ are strain invariants [7] and $\varepsilon_u$ is an ultimate total strain extrapolated from uniaxial test results. When $\varepsilon_u$ reaches the value specified as the ultimate strain, the material is assumed to lose all its characteristics of strength and rigidity.

## 2.2 Tensile behaviour of concrete

The response of concrete under tensile stresses is assumed to be linear elastic until the fracture surface is reached. This tensile type of fracture, or cracking, is governed by a maximum tensile stress criterion (tension cut-off). Cracks are assumed to form in planes perpendicular to the direction of maximum principal tensile stress as soon as this stress reaches the specified concrete tensile strength $f'_t$. After cracking has occurred, the elasticity modulus and Poisson's ratio are reduced to zero in the direction perpendicular to the cracked plane, and a reduced shear modulus, $G^c$, (based on the strain component normal to the crack) is employed.

Due to bond effects, cracked concrete carries between cracks, a certain amount of tensile force normal to the cracked plane. The concrete adheres to the reinforcing bars and contributes to the overall stiffness of the structure [8]. Several approaches based on experimental results have been employed to simulate this tension stiffening behaviour [9-11]. A gradual release of the concrete stress component normal to the cracked plane (Fig. 2) is adopted in this work. The process of loading and unloading of cracked concrete is also illustrated in Figure 2.

## 3. Transient thermal stress solution procedures

The solution technique described in this section involves concurrently solving an uncoupled set of equations (the transient heat conduction equations and the incremental equilibrium equations) within a time interval to provide both the temperature and displacement increments.

## 3.1 Transient temperature analysis

The temperature field $\underline{T}_n$ existing in the solid at any instant of time $t_n$ must satisfy the following equation system

$$\underline{K}(\underline{T}_n)\underline{T}_n + \underline{C}(\underline{T}_n)\,\dot{\underline{T}}_n + \underline{F}(\underline{T}_n, t_n) = 0 \tag{4}$$

in which $\underline{K}$ and $\underline{C}$ are respectively the thermal conductivity and heat capacity matrices, which may be temperature dependent, and $\underline{F}$ represents the thermal loading which may vary with respect to both temperature and time. Employing the usual two level scheme for the time discretisation of (4) results in the following expression for the variation of temperature within a time interval $\Delta t_n = t_{n+1} - t_n$,

$$\underline{T}_{n+\alpha} = |\hat{\underline{K}}_{n+\alpha}|^{-1}\,\hat{\underline{F}}_{n+\alpha} \tag{5a}$$

and

$$\underline{T}_{n+1} = \frac{1}{\alpha}\,\underline{T}_{n+\alpha} - (1 - \frac{1}{\alpha})\,\underline{T}_n \tag{5b}$$

where

$$\hat{\underline{K}}_{n+\alpha} = \underline{K}(\underline{T}_{n+\alpha}) + \underline{C}(\underline{T}_{n+\alpha}) \frac{1}{\alpha \Delta t_n} \tag{6a}$$

$$\hat{\underline{F}}_{n+\alpha} = \underline{F}(\underline{T}_{n+\alpha}, t_{n+\alpha}) + \underline{C}(\underline{T}_{n+\alpha}) \frac{1}{\alpha \Delta t_n} \underline{T}_n \tag{6b}$$

The appropriate choice of $\alpha$ in the range $0 \leq \alpha \leq 1$ results in various standard time integration algorithms.

3.2 Thermal stress determination

Thermal stress determination involves an elasto-viscoplastic time dependent material analysis accounting for both nonlinear compressive behaviour and tensile cracking effects. The onset of viscoplastic flow is governed by a scalar yield criterion of the form [12]

$$F(\underline{\sigma}, \chi) = f(\underline{\sigma}) - \sigma_o(\chi) \tag{7}$$

in which $\chi$ is a hardening parameter.

For associated viscoplasticity the viscoplastic strain rate is given by

$$\dot{\underline{\varepsilon}}_{vp} = \gamma \langle \phi \left( \frac{f - \sigma_o}{\sigma_o} \right) \rangle \frac{\partial f(\underline{\sigma})}{\partial \underline{\sigma}} \tag{8}$$

in which $\gamma$ is a fluidity parameter and $\langle \phi \rangle$ is the flow function taken as non-zero for $f > \sigma_o$ only.

Expressing the total strain in terms of the displacement increment $\Delta \underline{d}^n$ occurring in a time interval $\Delta t_n = t_{n+1} - t_n$ and the viscoplastic component according to an Euler forward difference representation results in

$$\Delta \underline{\sigma}^n = \underline{D}^n (\underline{B} \Delta \underline{d}^n - \dot{\underline{\varepsilon}}_{vp}^n \Delta t_n) - \Delta \underline{\sigma}_I^n \tag{9}$$

in which $\underline{B}$ is the usual strain-displacement matrix and $\underline{D}$ is the elasticity matrix modified to account for tensile cracking behaviour. The term $\Delta \underline{\sigma}_I^n$ in expression (9) represents the initial stress system associated with the temperature change occurring during the time interval $\Delta t_n$.

The incremental form of the equilibrium equations is

$$\int_\Omega \underline{B}^T \Delta \underline{\sigma}^n \, d\Omega = \Delta \underline{f}^n \tag{10}$$

in which $\Delta \underline{f}^n$ represents the change in equivalent nodal loads resulting from body forces and tractions occurring during the time interval $\Delta t_n$. Substituting from (9) in (10) results in the following expression for the displacement increment

$$\Delta \underline{d}^n = [\underline{K}_T^n]^{-1} \Delta \underline{V}^n \tag{11}$$

where the current stiffness matrix $\underline{K}_T^n$ is

$$\underline{K}_T^n = \int_\Omega \underline{B}^T \underline{D}^n \underline{B} \, d\Omega \tag{12}$$

and the incremental "pseudo loads", $\Delta \underline{V}^n$ are given by

$$\Delta \underline{V}^n = \Delta \underline{f}_{vp}^n + \Delta \underline{f}^n + \Delta \underline{f}_I^n \tag{13}$$

in which $$\Delta \underline{f}_{vp}^n = \int_\Omega \underline{B}^T \underline{D}^n \dot{\underline{\varepsilon}}_{vp}^n \Delta t_n \, d\Omega \tag{14a}$$

$$\Delta \underline{f}_I^n = \int_\Omega \underline{B}^T \underline{\sigma}_I^n \, d\Omega \tag{14b}$$

With all incremental values known, quantities can be updated to give the solution at time $t_{n+1}$.

The above time stepping procedure can be performed concurrently with the thermal process of Section 3.1 for as many time intervals as required.

## 4. Numerical Examples

Two numerical examples are presented in this section which illustrate the applicability of the numerical methods described in this paper.

### 4.1 Example I, thermal elasto-viscoplastic analysis of a thick walled cylinder

The problem is defined in Fig. 3 where it is seen that the cylinder is discretised by six 8-node Serendipity elements. Both the mechanical and thermal properties of the material are included and it is seen, in particular, that the yield stress is temperature dependent. The thermal boundary conditions are that the temperature at the inside surface is specified while a convective heat transfer condition is assumed at the outer face. The two lateral surfaces of the cylinder are assumed to be thermally insulated.

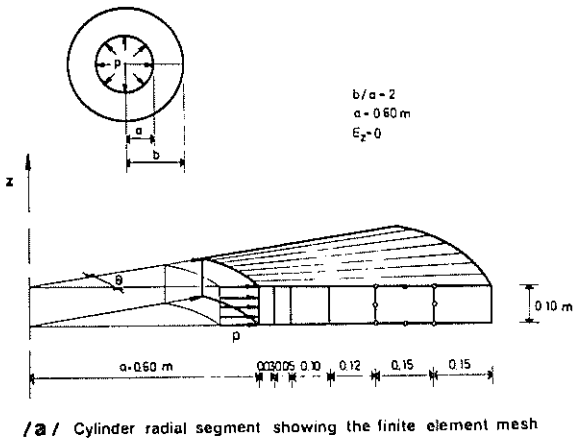


/a/ Cylinder radial segment showing the finite element mesh

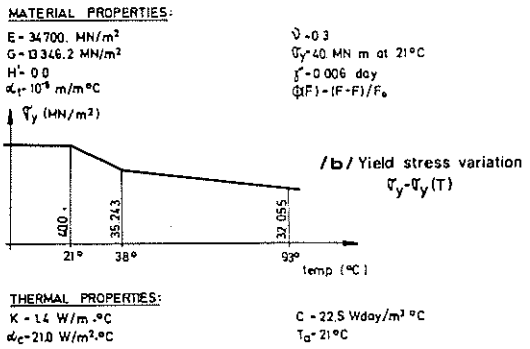


/b/ Yield stress variation $\sigma_y$-$\sigma_y$(T)

Fig. 3 Thermal elasto-viscoplastic thick walled cylinder (Example I)

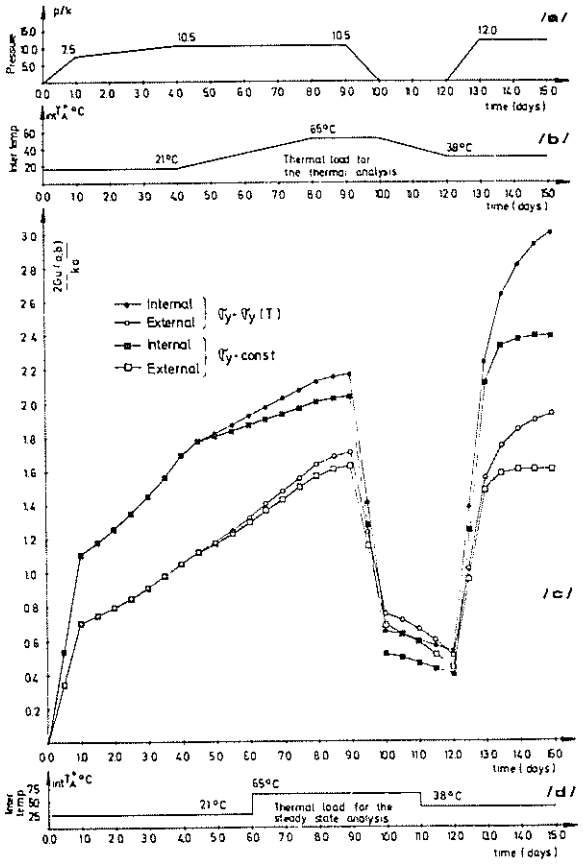


Fig. 4 Displacement response of the thick walled cylinder of Example I for different yield stress variations

Both the internal pressure and the temperature at the internal surface are varied with time as indicated in Fig. 4(a) and (b). The Galerkin time stepping scheme ($\alpha$ = 2/3) is employed for temperature analysis with a time step length $\Delta t$ = 0.5 day, which is within the oscillatoric

limit [13]. An explicit approach is considered for viscoplastic analysis for which the chosen time step length $\Delta t$ = 0.5 day satisfies the stability criterion of Ref. [14]. The effects of different uniaxial yield stress levels are investigated. In particular, comparison is made between solutions obtained using the yield stress variation of Fig. 3 and a constant value of 40.0 MN/m$^2$. These results are compared in Fig. 4(c) where the significant differences which are evident clearly indicate the importance of using accurate values of nonlinear material parameters.

## 4.2 Example II, thermal cracking of a prestressed concrete ring

The ring of internal radius 38.1 cm and external radius 50.8 cm is subjected to both a constant internal pressure and a transient thermal loading/unloading cycle as illustrated in Fig. 5. The problem parameters are listed in Table I. The ring is prestressed at time t=0 and a time step length $\Delta t$ = 0.25 hr is employed in solution. The Euler-Backward algorithm ($\alpha$=1) is considered for transient thermal analysis and the explicit approach of Section 3.2 used for the stress analysis.

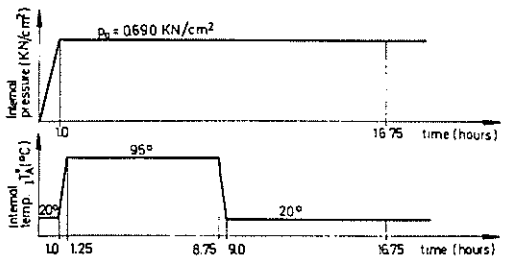


Fig. 5 Internal pressure and temperature variation with time for Example II

| MECHANICAL PARAMETERS | | | | | |
|---|---|---|---|---|---|
| CONCRETE | Elasticity modulus | $E_c$ = 2965. kN/cm² | Max. tension stiffening strain | $^{max}\varepsilon_t$ = 0.003 | |
| | Poisson's ratio | $\nu_c$ = 0.15 | Shear retention equivalent strain | $^{max}\varepsilon_{sh}$ = 0.002 | |
| | Compressive strength | $f'_c$ = 4.758 kN/cm² | | | |
| | Tensile strength | $f'_t$ = 0.345 kN/cm² | Ultimate compression strain | $\varepsilon_{cu}$ = 0.004 | |
| | Fluidity param. | $\gamma$ = 0.00025/hr | | | |
| | Flow function | $\phi(\bar{F})$ = $(F - F_0)/F_0$ | Thermal expansion parameter | $^c\alpha_t$ = 0.00001 | |
| STEEL | Elasticity modulus | $E_s$ = 19306 kN/cm² | Area of hoop cable | A = 0.187 cm² | |
| | Yield stress | $\sigma_y$ = 155.0 kN/cm² | Hoop cable spacing | 1 cable /0.85 cm | |
| | Equivalent yield stress | $^{eq}\sigma_y$ = 55.85 kN/cm² | Equivalent thickness of hoop membrane | $t_s$ = 2.21 cm | |
| | Thermal expansion parameter | $^s\alpha_t$ = 0.00001 | | | |

| THERMAL PARAMETERS | | |
|---|---|---|
| Heat conductivity | K = 0.014 | W/cm-°C |
| Heat capacity | C = 0.00054 | Wsec/cm³-°C |
| Convection coeff. | $a_c$ = 0.0021 | W/cm²-°C |
| External ambiental temperature | $^{ex}T_\theta$ = 20°C | |
| Initial temperature | $T_0$ = 20°C | |

| PRESTRESSING | | | |
|---|---|---|---|
| Total axial prestressing force | $P_z$ = 3363. kN | Hoop prestressing force per cable | $P_h$ = 18.577 kN |
| Equivalent vertical restrain | $^{eq}\varepsilon_z$ = 0.002012 cm | Equivalent external pressure | $^{eq}P_h$ = 0.508 kN/cm² |

Table I Problem parameters for Example II

In addition to the thermal loading shown in Fig. 5 an analysis was also performed in which the steady state temperature distributions corresponding to prescribed internal temperatures of 95° and 20°C were assumed to be instantaneously achieved and these were then used for stress determination in the concrete. These two approaches predict significantly different thermal cracking histories for the concrete as shown in Fig. 6. No cracks are produced under prestressing and internal pressure loading. Using the full transient thermal response in analysis, the first radial cracks appear at time t=1.25 hours when the increased internal temperature causes tensile thermal stress near the external surface and compensating compressive components near the inner surface. After thermal unloading at t = 9.0 hours, these cracks become closed, but new radial cracks are formed at the internal surface. Finally all the cracks in the ring become gradually closed as the temperature in the ring approaches the steady state condition at t=16.75 hours.

## 5. Discussion of results and conclusions

Finite element techniques have been presented for the nonlinear analysis of reinforced and prestressed concrete components and structures and the numerical examples presented

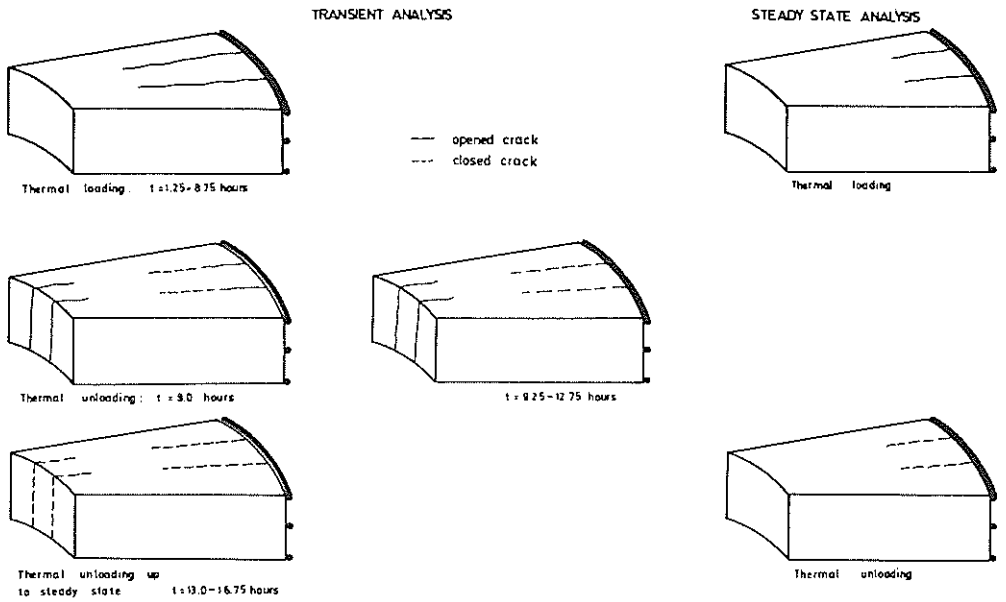


Fig. 6 Cracking history for the prestressed ring of Example II

illustrate the applicability of the methods. Moreover the nonlinear solution process proved to be both robust and computationally economic.

It is claimed in Ref. [15] that for the numerical analysis of tensile softening materials, a judicious choice of element dimensioning is required in order to ensure convergence to the correct solution. Numerical experiments conducted with successively refined meshes did not indicate the solution convergence characteristics to be significantly influenced by this factor for the problems considered.

## 6. References


1. ASCE Committee on concrete and masonry structures, Task Committee on Finite Element Analysis of Reinforced Concrete Structures: A State-of-the-Art Report on Finite Element Analysis of Reinforced Concrete Structures, ASCE Spec. Pub. 1981.
2. W. C. SCHNOBRICH
   Behaviour of reinforced concrete structures predicted by the finite element method, Computers & Structures, Vol. 7, pp. 365-376, 1977.
3. J. H. ARGYRIS, G. FAUST, J. SZIMMAT, E. P. WARNKE and K. J. WILLAM
   Recent developments in the finite element analysis of prestressed concrete reactor vessels, Nuclear Engineering and Design, 28, pp. 42-75, 1974.
4. P. G. BERGAN and I. HOLAND
   Nonlinear finite element analysis of concrete structures, Computer Methods in Applied Mechanics and Engineering, 17/18, pp. 443-467, 1979.
5. K. H. GERSTLE
   Material modelling of reinforced concrete, Introductory Report, IABSE Colloquium on Advanced Mechanics of Reinforced Concrete, Delft, Volume-Band 33, pp. 41-63, 1981.
6. H. KUPFER, K. H. HILSDORF and H. RUSH
   Behaviour of concrete under biaxial stresses, Proceedings, American Concrete Institute, Vol. 66, No.8, pp. 656-666, August, 1969.
7. W. F. CHEN
   Plasticity in Reinforced Concrete. McGraw-Hill Book Company, 1982.

8. Y. GOTO
Cracks formed in concrete around deformed tension bars, ACI Journal, April 1971, pp. 244-251.

9. C. S. LIN and A. C. SCORDELIS
Nonlinear analysis of RC shells of general form, ASCE Journal of the Structural Division, Vol. 101, No.ST3, March 1975, pp. 523-538.

10. R. I. GILBERT and R. F. WARNER
Tension stiffening in reinforced concrete slabs, ASCE Journal of the Structural Division, Vol. 104, No. ST12, December 1978, pp. 1885-1900.

11. R. J. COPE, P. V. RAO, L. A. CLARK and P. NORRIS
Modelling of reinforced concrete behaviour for finite element analysis of bridge slabs. Numerical Meth. for Nonlinear Problems, Vol. 1, Pineridge Press. Proceedings of the International Conference held at University College of Swansea, 2-5 September 1980, pp. 457-470.

12. D. R. J. OWEN and E. HINTON
Finite Elements in Plasticity - Theory and Practice. Pineridge Press, Swansea, U.K. 1980.

13. F. DAMJANIC and D. R. J. OWEN
Practical considerations for thermal transient finite element analysis using isoparametric elements. Nuc. Eng. & Design, Vol. 69, No.1, 109-126, 1982.

14. D. R. J. OWEN and F. DAMJANIC
Viscoplastic analysis of solids: Stability considerations, Chapter 8 in "Recent Advances in Nonlinear Computational Mechanics" (Ed. E. Hinton et al.), Pineridge Press, U.K. 1982.

15. Z. P. BAZANT
Crack band model for fracture of geomaterials. Proc. 4th Int. Conf. Num. Methods in Geomechanics, Edmonton, Canada, May 1982.